

Reflection of Light from Semi-Infinite Absorbing Turbid Media. Part 1: Spherical Albedo

Alexander A. Kokhanovsky,^{1*}
Leonid G. Sokoletsky^{2†}

¹Institute of Environmental Physics, University of Bremen, Otto Hahn Alee 1, D-28334 Bremen, Germany

²Israel Oceanographic and Limnological Research, Yigal Allon Kinneret Limnological Laboratory, P.O. Box 447, Migdal 14950, Israel

Received 15 April 2005; accepted 5 January 2006

Abstract: The purpose of this article is to study the accuracy of a number of simple approximate equations for the spherical albedo r (or the hemispherical reflectance under diffuse illumination conditions) of semi-infinite light scattering absorbing media, using numerical solutions of the nonlinear integral equation for the reflection function of a semi-infinite turbid medium, as formulated by V. A. Ambartsumian. We find that the van de Hulst approximation provides the most accurate approximation for the diffuse reflectance r under diffuse illumination conditions. The value of r depends almost exclusively on the value of the similarity parameter $s = \sqrt{(1 - \omega_0)(1 - g\omega_0)^{-1}}$, where ω_0 is the single scattering albedo and g is the asymmetry parameter.

A simple approach to derive the normalized absorption spectra of particulate matter from reflectance measurements is proposed. © 2006 Wiley Periodicals, Inc. *Col Res Appl*, 31, 491–497, 2006; Published online in Wiley InterScience (www.interscience.wiley.com). DOI 10.1002/col.20262

Key words: color matching; color modeling; radiometry and photometry; radiative transfer

INTRODUCTION

The problem of light interaction with a turbid medium is of great importance for various technological applications including the creation and improvement of color-matching programs,

which are widely used in paint, plastics, and textile laboratories.¹ Usually, the Kubelka–Munk² approximation (KMA) is used as a main theoretical tool for technological applications. As emphasized by Pierce and Marcus,¹ excellent matches could be made for light and medium shade solid colors, using KMA. However, problems arise for dark colors. Also, KMA is not capable of dealing with directional quantities (e.g., the bidirectional reflection function). Then one needs to use more elaborate approaches based on the radiative transfer theory.³ This theory is not widely used in technological laboratories (primarily, because of its complexity). However, in recent years, a number of approximate results were formulated, which, having almost the same level of simplicity as KMA, offer a better accuracy and a greater range of applicability of analytical equations derived. An excellent review of the theory as far as isotropic scattering is of concern was given by Pierce and Marcus.¹ A comprehensive bibliographical review containing 132 references was prepared by Phillips-Invernizzi *et al.*⁴

This article is composed of five sections. Main Definition and Phase Function sections are aimed to describe the main definitions and the description of single scattering laws used in this study, respectively. We discuss the various approximations for the spherical albedo in the Spherical Albedo section. The main concern of the Similarity Parameter section is the study of the possibility of deriving the spectral absorption coefficient of particulates from spectral reflectance measurements. We also discuss the problem of color optimization using equations presented.

MAIN DEFINITIONS

Reflectance spectroscopy is a major remote-sensing technique used to study chemical composition and microstruc-

*Correspondence to: Alexander A. Kokhanovsky (e-mail: alexk@iup.physik.uni-bremen.de)

†Current Address: Department of Environmental Sciences and Energy Research, The Weizmann Institute of Science, Rehovot 76100, Israel.

Contract grant sponsor: DFG, Contract grant number: DFG 688/8–1.
© 2006 Wiley Periodicals, Inc.

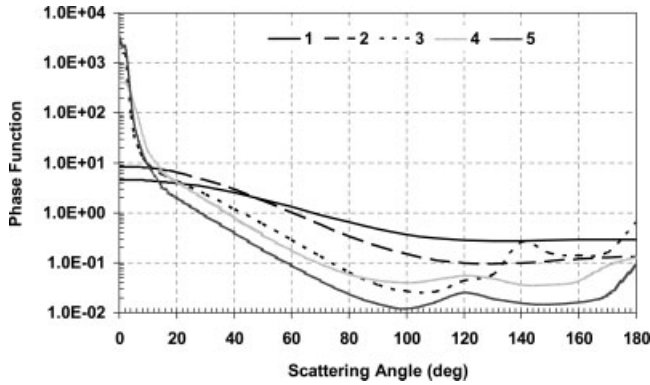


FIG. 1 Phase functions used for calculations (numbers correspond to those in Table I).

ture of various light scattering media. The reflected light spectrum is measured and used to decode the relevant information with respect to inherent properties of a turbid layer in the framework of the radiative transfer theory.⁵ Also, this theory is important for understanding optical properties, appearance, and design of various paints, foams, fabrics, and plastics.

In many cases, the scattering medium of interest has a large optical thickness τ and, therefore, can be treated as a semi-infinite turbid layer. Then the intensity of reflected light depends on the probability of photon survival in a single scattering event ω_0 and the phase function $p(\theta)$. The phase function gives a probability of photon scattering in a given direction.

Of course, there is also the dependence on the geometry of the problem if one is interested in the bidirectional reflectance and not in its integrated value (e.g., illumination (ϑ_0) and viewing (ϑ) angles, and the relative azimuth φ). For specific applications, one must account for additional factors like the ratio between incoming diffuse and direct irradiance fluxes, and specific boundary conditions. For instance, optical processes occurring at the air–water interface^{6–8} are of great importance in the area of ocean optics. Surface reflection corrections as used in color matching are described in detail by Pierce and Marcus.¹ Therefore, they will be not considered here. However, we note that the account for the boundary surface reflection contribution (e.g., from a resin film, where pigments are embedded) can be easily done, if needed.

Theoretical reflectance spectra for a semi-infinite turbid medium can be obtained by solving the nonlinear integral equation derived by Ambartsumian,⁹ using the invariance principles. However, such an approach is not suitable for the inverse problem solution, because of the computational burden. Therefore, approximate results have been proposed to calculate the turbid medium reflection characteristics, including the spherical albedo, the plane albedo, and the reflection function.

The reflection function $R(\xi, \eta, \varphi)$ (ξ is the cosine of the incidence angle ϑ_0 , η is the cosine of the observation angle ϑ , φ is the relative azimuth) is defined as the ratio of the intensity of light reflected from a given turbid layer to the

intensity of light reflected from the Lambertian absolutely white surface. Therefore, it follows $R = 1$ for the Lambertian absolutely white surface by definition. The plane albedo $\mathfrak{R}(\xi)$ can be derived from the following equation:

$$\mathfrak{R}(\xi) = \frac{1}{\pi} \int_0^{2\pi} \int_0^1 R(\xi, \eta, \varphi) \eta \, d\eta \, d\varphi. \quad (1)$$

We see that the value of \mathfrak{R} gives the diffuse reflectance under directional illumination of a turbid layer. It follows for the spherical albedo r by definition:

$$r = 2 \int_0^1 \mathfrak{R}(\xi) \xi \, d\xi. \quad (2)$$

The physical meaning of r is the same as \mathfrak{R} , except for the diffuse light illumination conditions.¹⁰ Note that it follows from the conservation energy law: $r = 1$ and also $\mathfrak{R}(\xi) = 1$ at any ξ for nonabsorbing semi-infinite media.^{10,11} This means that photons cannot accumulate in the medium and must return back in outer space, where a light source is located.

Next sections are devoted to a critical review of selected most accurate approximate results for the spherical albedo of a plane-parallel homogeneous turbid layer. Their accuracy is accessed by solving the exact radiative transfer equation as described by Mishchenko *et al.*¹²

PHASE FUNCTIONS

The phase function describes the angular distribution of scattered light in a single scattering event. This function must be used as an input for the radiative transfer calculations. Five different phase functions have been selected for this study (Fig. 1). They have been calculated using Mie theory for the gamma particle size distribution (PSD)

$$f(a) = A \exp(-9a/a_{ef}) \quad (3)$$

at the wavelength $\lambda = 0.55 \mu\text{m}$ for different values of the effective radius a_{ef} and refractive indices $m = n - i\chi$, as specified in Table I. Here A is the normalization constant ($\int_0^\infty f(a) da = 1$) and a is the radius of a spherical particle.¹¹ Correspondent asymmetry parameters g and backward fractions B defined as

$$g = \frac{1}{2} \int_0^\pi p(\theta) \sin\theta \cos\theta \, d\theta, \quad B = \frac{1}{2} \int_{\pi/2}^\pi p(\theta) \sin\theta \, d\theta \quad (4)$$

TABLE I. Parameters used in Mie calculations and results for the pair (g, B).

| N | $a_{ef} (\mu\text{m})$ | n | χ | g | B |
|-----|------------------------|------|--------|--------|--------|
| 1 | 0.116 | 1.25 | 0.001 | 0.5033 | 0.1559 |
| 2 | 0.175 | 1.25 | 0.001 | 0.6962 | 0.0589 |
| 3 | 6 | 1.33 | 0.0 | 0.8546 | 0.0407 |
| 4 | 2 | 1.2 | 0.01 | 0.9062 | 0.0229 |
| 5 | 5 | 1.2 | 0.01 | 0.9583 | 0.0087 |

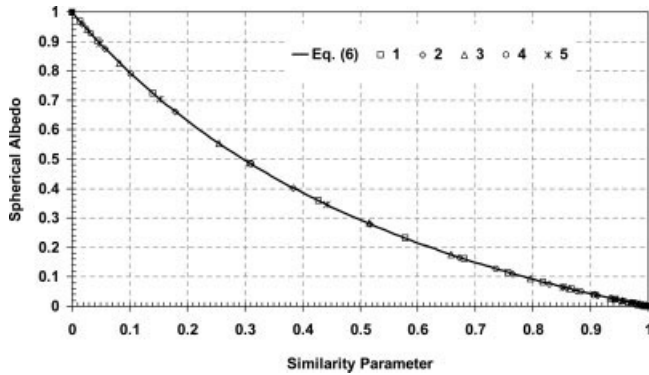


FIG. 2 Dependence of the spherical albedo on the similarity parameter (solid curve—Eq. (6), symbols—exact calculations for different phase functions and single scattering albedos (numbers correspond to those in Table I).

are given in Table I as well. These parameters are often used in the parameterizations of reflection characteristics. Yet another important parameter (“similarity parameter” as it was named by van de Hulst^{13,14}) is calculated as

$$s = \sqrt{\frac{1 - \omega_0}{1 - g\omega_0}}. \quad (5)$$

It was found that the spherical albedo r is governed mostly by the value of s independently on the phase function.^{13,14}

Selected phase functions are very diverse with respect to the values of g , B , and the forward–backward asymmetry.¹⁵ The phase functions (1) and (2) weakly vary with the scattering angle and are typical for white pigments and red dyes used in color matching.^{16,17} The phase function (3) as shown in Fig. 1 is typical for terrestrial water clouds.¹¹ In particular, a rainbow feature around the scattering angle of 140° is clearly seen for this curve. Additionally, the phase functions (2) and (3) are typical ones for clear oceanic waters, whereas highly extended in the forward direction phase functions (4) and (5) are more relevant for describing more turbid waters and biological tissues.¹¹ These diverse phase functions are well suited for the studies of the accuracy of various approximations. Although Mie calculations also provide the single scattering albedo for a given PSD and the refractive index $m = n - i\chi$, we used predefined values of ω_0 ranging from 0.0 to 1.0, with the step 0.1 in the radiative transfer calculations for phase functions shown in Table I.

SPHERICAL ALBEDO

The convenient and simple equation for the spherical albedo of a semi-infinite light scattering medium was proposed by van de Hulst¹³:

$$r = \frac{(1 - s)(1 - hs)}{1 + qs}. \quad (6)$$

where $h = 0.139$ and $q = 1.17$. The van de Hulst approximation (HA) suggests that one can neglect the influence of a particular phase function on the total reflectance integrated

over incidence and observation directions. The value of r is mostly governed by the similarity parameter s , independently on particular values of g and ω_0 . Thus, spectral measurements of r allow to determine the similarity parameter spectrum $s(\lambda)$. Namely, we have from Eq. (6)

$$s(\lambda) = \frac{(1 + h + qr(\lambda))(1 - \sqrt{1 - w(\lambda)})}{2h}, \quad (7)$$

where $w(\lambda) = 4(1 - r(\lambda))(1 + h + qr(\lambda))^{-2}h$. This reduces the problem of the microstructure/chemical composition determination for an optically thick turbid layer to that for the elementary volume of a scattering medium. Single scattering theories must be used to derive, e.g., the spectral variation of the refractive index from the spectrum $s(\lambda)$. We will touch upon this problem in the next section.

The results of calculations according to Eq. (6) and also the results of our exact radiative transfer simulations using the radiative transfer code as described by Mishchenko *et al.*¹² are shown in Fig. 2. It follows that Eq. (6) accurately represents the dependence $r(s)$ for all phase functions studied (Fig. 1). This means that reflectance measurements can be used to derive s [e.g., see Eq. (7)] and, therefore, to reduce the multiple scattering inverse problem to the single scattering one. In particular, the spectrum $s(\lambda)$ is easily simulated using Mie theory for spherical particles.¹¹ The relative error δ of Eq. (6) is shown in Fig. 3. It follows that δ is larger for smaller values of r (dark media). However, there is no error at $s = 1$, where $r = 0$, and a medium does not reflect light at all. Clearly such conditions do not occur in practice. The error is smaller than 1% at $s < 0.75$ or $r > 0.15$. This range of r is typical for many artificial and natural surfaces in visible and infrared with exception of natural waters, where r is usually below 0.15. So Eq. (6) is of importance for practical applications. The accuracy of Eq. (6) is better than 7% for all phase functions and single scattering albedos ($s \in [0, 1]$) studied in this work.

There is yet another accurate approximation for the spherical albedo^{16,17}:

$$r = 1 + \gamma - \sqrt{(2 + \gamma)\gamma} \quad (8)$$

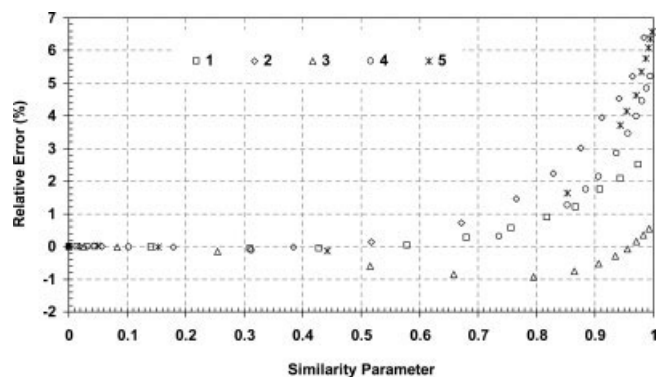


FIG. 3 Relative errors of Eq. (6) for the different phase functions and similarity parameters (numbers correspond to those in Table I).

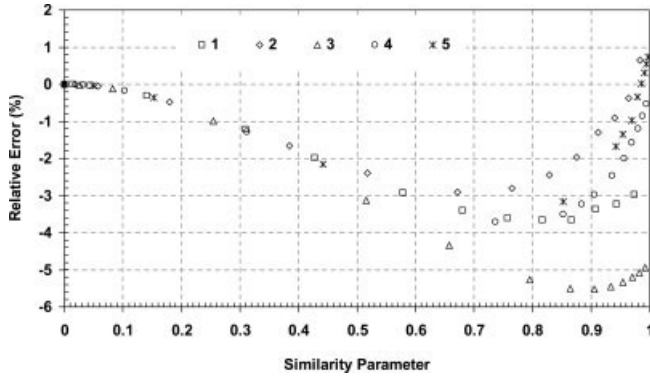


FIG. 4 Relative errors of Eq. (8) with account for Eq. (9) for the different phase functions and similarity parameters (numbers correspond to those in Table I).

with $\gamma = 8(1 - \omega_0)/3\omega_0(1 - g)$. We find that the value of γ can be also rewritten as

$$\gamma = \frac{8}{3} \frac{s^2}{1 - s^2}, \quad (9)$$

thereby reducing the number of parameters in the expression for γ to just one. Historically, Eq. (8) was proposed by Kubelka and Munk.² However, they considered only the isotropic scattering ($g = 0$) case, and did not provide the relationship between γ and g [or s , see Eq. (9)]. We call the combination of Eqs. (8) and (9) the modified Kubelka–Munk approximation (MKMA).

As a matter of fact, Eq. (9) is quite important, because it provides a way to calculate γ exactly (e.g., using Mie theory¹⁸) not referring to a poorly defined Kubelka–Munk ratio K/S .¹⁹

The relative error of MKMA is given in Fig. 4. The plot of the spherical albedo as a function of s in this approximation is very close to that shown in Fig. 2. The errors of Eq. (8) with account for Eq. (9) are small (Fig. 4). They are less than 6% for all $s \in [0, 1]$. However, the distribution of errors with s differs from that for the van de Hulst approximation (compare Figs. 3 and 4). We see that Eq. (8) with s given by Eq. (9) has generally somewhat smaller errors as $r \rightarrow 0$ as compared to the van de Hulst approximation. This peculiarity is important for aquatic optics applications, especially in the cases where a content of solid particles in the water column is insignificant.²⁰ The derivation of Eq. (8) and more discussions on the applicability of this and other similar approximations can be found elsewhere.^{5,11,16,17,21,22}

We note that it follows from Eqs. (8) and (9)

$$s = \sqrt{\frac{3\gamma}{3\gamma + 8}} \quad (10)$$

and

$$s(\lambda) = (1 - r(\lambda)) \sqrt{\frac{3}{16r(\lambda) + 3(1 - r(\lambda))^2}}. \quad (11)$$

Therefore, as in the case of the van de Hulst approximation,

TABLE II. The values of spherical albedo r in the framework of different approximations (r_1 (MKMA) and r_2 (HA)) for different s .

| s | r_1 | r_2 | δ (%) |
|-----|-------|-------|--------------|
| 0.0 | 1.000 | 1.000 | 0.000 |
| 0.1 | 0.793 | 0.795 | 0.158 |
| 0.2 | 0.627 | 0.630 | 0.553 |
| 0.3 | 0.491 | 0.497 | 1.101 |
| 0.4 | 0.379 | 0.386 | 1.740 |
| 0.5 | 0.286 | 0.294 | 2.423 |
| 0.6 | 0.209 | 0.215 | 3.113 |
| 0.7 | 0.143 | 0.149 | 3.782 |
| 0.8 | 0.088 | 0.092 | 4.411 |
| 0.9 | 0.040 | 0.043 | 4.984 |
| 1.0 | 0.000 | 0.000 | 0.000 |

The relative difference δ is defined as $\delta = 100(1 - r_1/r_2)$. The value of δ for the exponential approximation is smaller than 2% at $s \leq 0.3$.

one can easily derive the spectrum of $s(\lambda)$ from the reflectance spectrum $r(\lambda)$ and vice versa.

It follows from Figs. 3 and 4 that Eqs. (6) and (8) have almost the same accuracy as $s \rightarrow 1$. However, the accuracy of Eq. (6) is better for bright materials, when $s \rightarrow 0$ (Fig. 3). Therefore, we advise the use of the van de Hulst approximation for technological applications, and especially for color matching procedures. Results of calculations using Eqs. (6) and (8) [with account for Eq. (9)] are compared in Fig. 5. We also show the exponential approximation (EA) for r derived by Bushmakova *et al.*²³:

$$r = \exp(-\sigma s) \quad (12)$$

where $\sigma = 4/\sqrt{3}$, in Fig. 5. It follows that HA, MKMA, and EA differ one from another not more than by 2% at $s \leq 0.3$. For larger s , the EA deviates considerably from both modified KMA and HA. Maximal differences of modified KMA and HA reach 3% in the interval $0.3 \leq s \leq 0.7$ (Table II). They are somewhat larger at larger s and can reach 5% as shown in Table II. However, then both approximations have a reduced accuracy (Figs. 3 and 4). This means that for very dark materials, one needs to account for the phase function effects. The parameter s alone is not able to provide a high accuracy in this case. The physical back-

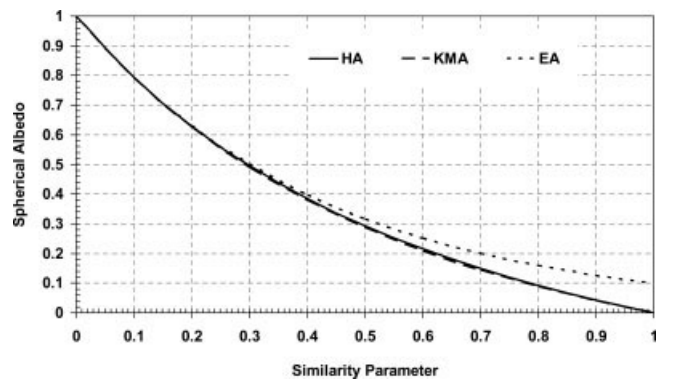


FIG. 5 Dependence of the spherical albedo on the similarity parameter s , as calculated using HA (solid line), MKMA (dashed line), and EA (dotted line) (see also Table II).

ground of this effect is obvious. Indeed, the parameter s is important for multiple light scattering effects. However, single scattering, and, therefore, the phase function plays a major role as $s \rightarrow 1$ ($\omega_0 \rightarrow 0$). This is not accounted for in either modified KMA or HA. The approach to treat this special case must be based on the single scattering approximation and its extensions^{11,24}.

SIMILARITY PARAMETER

The similarity parameter s is of crucial importance for reflectance problems. In particular, it is relatively easy to derive this parameter from reflectance spectra $r(\lambda)$ and also, knowing the spectrum $s(\lambda)$, one can easily predict the spectrum $r(\lambda)$ as shown in the previous section. Therefore, relations given earlier are very important for a number of technological applications and, in particular, for design and optimization of colors in textile laboratories and paint industry. In particular, if one is interested in having a given color of a turbid layer, one must find $s(\lambda)$ for a desired $r(\lambda)$ as shown earlier. This reduces the multiple light scattering problem to a single scattering one. Therefore, spectra $\omega_0(\lambda)$ and $g(\lambda)$ must be optimized in such a way that the desired spectrum $s(\lambda)$ [see Eq. (5)] is obtained. The optimization must be performed with respect to the size, shape, structure, and chemical composition of scattering elements (e.g., liquid or solid particles) and correspondent additives (e.g., dyes).

Spectral dependencies $\omega_0(\lambda)$ and $g(\lambda)$ [and therefore $s(\lambda)$] can be relatively easily simulated for ensembles of spherical scatterers. In particular, the following relationships hold^{18,25}:

$$\omega_0(\lambda) = 1 - \frac{\sigma_{\text{abs}}(\lambda)}{\sigma_{\text{ext}}(\lambda)}, \quad (13)$$

$$\sigma_{\text{abs}} = N \int_0^\infty C_{\text{abs}}(a, \lambda) f(a) da, \quad (14)$$

$$\sigma_{\text{ext}} = N \int_0^\infty C_{\text{ext}}(a, \lambda) f(a) da, \quad (15)$$

$$g = \frac{\int_0^\infty G(a, \lambda) C_{\text{sca}}(a, \lambda) f(a) da}{\int_0^\infty C_{\text{sca}}(a, \lambda) f(a) da}. \quad (16)$$

Here N is the number of particles in a unit volume of a turbid layer, C_{abs} is the absorption cross section of a single sphere of the radius a and the refractive index $m = n - i\chi$, C_{sca} is the scattering cross section, and $C_{\text{ext}} = C_{\text{sca}} + C_{\text{abs}}$ is the extinction cross section. The value of $G(a, \lambda)$ gives the asymmetry parameter of a single sphere with the radius a . There are analytical equations to calculate cross sections and also G for spheres. It follows^{18,26}

$$C_{\text{sca}} = \frac{\pi}{k^2} \sum_{j=0}^{\infty} (2j+1)[|a_j|^2 + |b_j|^2], \quad (17)$$

$$C_{\text{ext}} = \frac{\pi}{k^2} \sum_{j=0}^{\infty} (2j+1)\text{Re}[a_j + b_j], \quad (18)$$

$$G = \frac{4\pi}{k^2 C_{\text{sca}}} \sum_{j=1}^{\infty} \left[\frac{j(j+2)}{j+1} \text{Re}\{a_j a_{j+1}^* + b_j b_{j+1}^*\} + \frac{2j+1}{j(j+1)} \text{Re}\{a_j b_j^*\} \right], \quad (19)$$

where $k = 2\pi/\lambda$. These equations reduce the calculations of cross sections and G to the summation of series. The number of terms required in series is close to the size parameter $x = ka$. The algorithms for the calculation of amplitude coefficients $a_j(x, m)$ and $b_j(x, m)$ are available on the internet.¹¹ Similar but more complex equations exist for nonspherical scatterers (see e.g., Asano and Yamamoto²⁷ and Mischenko *et al.*²⁸).

The system of equations given earlier can be used for the optimization of the spectrum $s(\lambda)$ (and therefore $r(\lambda)$ and also color) for the case of spherical particles, depending on their size distribution $f(a)$ and the refractive index m . The refractive index (and especially its imaginary part) can be easily modified using additives such as dyes having various spectral properties.

Scattering media of interest are very often composed of nonspherical particles of very complex and irregular shapes (e.g., fabrics and colored foams). Then the theoretical way for the optimization of spectral properties as underlined earlier becomes too involved to be handled even by the latest generations of computers. Physical insights in the problem are needed for further advancements. This enables shortcuts from the fundamental physics of the problem directly to technological applications. In particular, simple models for the simulation of spectra $s(\lambda)$ for arbitrarily shaped particles are needed. One of such models valid for weakly absorbing media with large particles is presented here.

Therefore, we assume that $ka \rightarrow \infty$ and $2\alpha a \rightarrow 0$, where $\alpha = 4\pi\chi(\lambda)/\lambda$. In this case the following relationship holds²⁹:

$$C_{\text{abs}}(\lambda) = \zeta\alpha(\lambda)V, \quad (20)$$

where V is the volume of a particle and the parameter ζ is only weakly sensitive to the wavelength. Basically, ζ depends on the shape of particles and on the real part of the refractive index n , which has no significant variation far from absorption bands of a given substance. We found using geometrical optics calculations that it follows for spheres and hexagonal cylinders: $\zeta = 1.27$ and $\zeta = 1.67$, respectively (at the refractive index $n = 1.3$ and aspect ratios of cylinders in the range 0.5–2.0). The substitution of Eq. (20) into Eq. (14) gives

$$\sigma_{\text{abs}} = N\zeta\alpha \int_0^\infty V(\vec{a}) f(\vec{a}) d\vec{a}, \quad (21)$$

where the multidimensional vector \vec{a} represents microphysical properties of a nonspherical particle (e.g., the aspect ratio, the circularity parameter, etc.) and V is its volume. Let us introduce the volumetric concentration c :

$$c = N \int_0^\infty V(\vec{a}) f(\vec{a}) d\vec{a}. \quad (22)$$

Then it follows:

$$\sigma_{\text{abs}} = c\zeta\alpha \quad (23)$$

for an elementary volume containing arbitrarily shaped particles, if conditions specified earlier are valid. Clearly, for media without any scatterers, we must have $\sigma_{\text{abs}} \equiv \alpha$, where we used $c = 1$. This means that ζ must be close to one (independently on λ) for arbitrarily shaped optically soft particles with the refractive index close to the refractive index of a surrounding medium.

The next important point we are going to use is the fact that both σ_{ext} and g for large weakly absorbing particles are almost spectrally neutral and $\sigma_{\text{ext}} = 1.5c\alpha_{\text{ef}}^{-1}$ (Ref. 11). Here $\alpha_{\text{ef}} = 3\bar{V}/\bar{S}$ is the effective radius of particles, \bar{S} is the average surface area of particles, and \bar{V} is their average volume. Summing up, we have for the similarity parameter [see Eq. (5)]

$$s(\lambda) = \Lambda \sqrt{\zeta\alpha(\lambda)\alpha_{\text{ef}}} \quad (24)$$

where we assumed that $\omega_0 \rightarrow 1$ and

$$\Lambda = \sqrt{\frac{2}{3(1-g)}} \quad (25)$$

only weakly depends on the wavelength. This allows us to obtain the following approximate relationship valid for media with arbitrarily shaped large weakly absorbing particles (e.g., as those appeared in fabrics and colored foams): $\alpha_n(\lambda) \approx s_n^2(\lambda)$, where $\alpha_n(\lambda) \equiv \alpha(\lambda)/\alpha(\lambda_0)$ and $s_n(\lambda) \equiv s(\lambda)/s(\lambda_0)$, and we neglected the dependence of Λ and ζ on the wavelength. Here λ_0 is an arbitrary wavelength from the interval, where $ka_{\text{ef}} \rightarrow \infty$, but $2\alpha a_{\text{ef}} \rightarrow 0$ as specified earlier. This allows to relate the desired spectrum $s(\lambda)$ [and therefore $r(\lambda)$] with a correspondent spectrum $\alpha(\lambda)$ using a simple analytical equation. The theory given earlier is only valid for weakly absorbing particles in nonabsorbing host media. The generalization of this theory for more complex cases can be easily done. For instance, if a dye is added to the substance of particles, then α in Eq. (24) must be substituted by $(1 - c_d)\alpha_p + c_d\alpha_d$, where α_p is the absorption coefficient of the substance from which particles are made, α_d is the dye absorption coefficient, and c_d is the concentration of a dye. An important case is that of $\alpha_p = 0$. Then it follows from Eq. (24)

$$s(\lambda) = \Lambda^* \sqrt{c_d\alpha_d(\lambda)\alpha_{\text{ef}}}, \quad (26)$$

where $\Lambda^* = \Lambda\sqrt{\zeta}$. This means that γ as given by Eq. (9) is linearly proportional to c_d only as $s \rightarrow 0$. It follows in the case of multiple colorants:

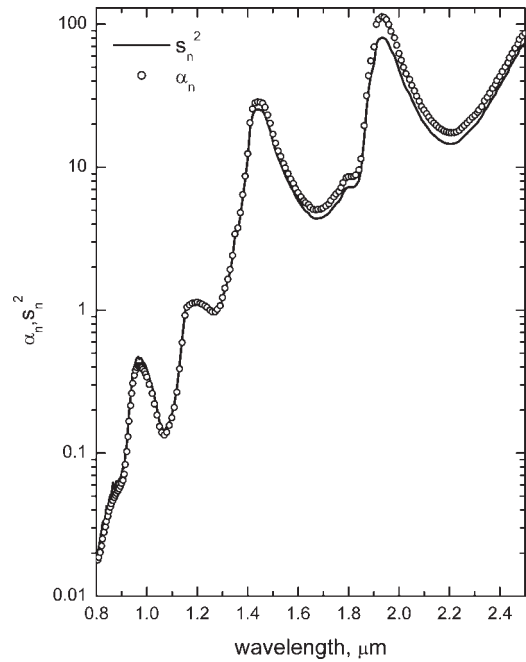


FIG. 6 Spectral dependence of α_n and s_n^2 for spherical polydispersions of water droplets (see details in the text).

$$s(\lambda) = \Lambda^* \sqrt{\sum_{i=1}^l c_{di}\alpha_{di}(\lambda)\alpha_{\text{ef}}}, \quad (27)$$

where l is the total number of dyes or colorants in a mixture and the index i refers to the i -th colorant. The value of l is taken to be equal to 3 for computer color matching applications (CMA).^{30,31} The application of Eqs. (6) and (27) for CMA (e.g., the choice of concentrations c_{di} to have a desired color) is straightforward. In particular, all derivatives as required by a tristimulus match technique³¹ can be derived analytically. We will not discuss this issue at any length here.

Instead, we check our chain of arguments for the special case of spherical particles. We have performed Mie calculations of the spectrum $s_n^2(\lambda)$ and also $\alpha_n(\lambda)$ for an ensemble of water spheres with the spectral refractive index as tabulated by Segelstein³² and the PSD (3) at $a_{\text{ef}} = 4 \mu\text{m}$. The normalization as discussed earlier has been performed at $\lambda_0 = 1.25 \mu\text{m}$.

The results of these exact calculations based on Eqs. (13)–(19) are shown in Fig. 6. We find that the spectrum $s_n^2(\lambda)$ follows very closely the correspondent spectrum $\alpha_n(\lambda)$. In particular, the positions of characteristic water bands coincide in both spectra. Therefore, our approach can indeed be used for the solution of a number of problems and in particular for the spectroscopy of turbid media, color design, and chemical composition identification using reflectance measurements.

We show the difference $\Delta = 100(1 - s_n^2/\alpha_n)$ as the function of the wavelength in Fig. 7. The value of Δ is smaller than 10% at $\lambda \leq 1.4 \mu\text{m}$. The difference increases for larger λ , because conditions $ka_{\text{ef}} \rightarrow \infty$ and $Y = 2\alpha a_{\text{ef}} \rightarrow 0$ are only partially met then for the specific case considered here. In particular, it

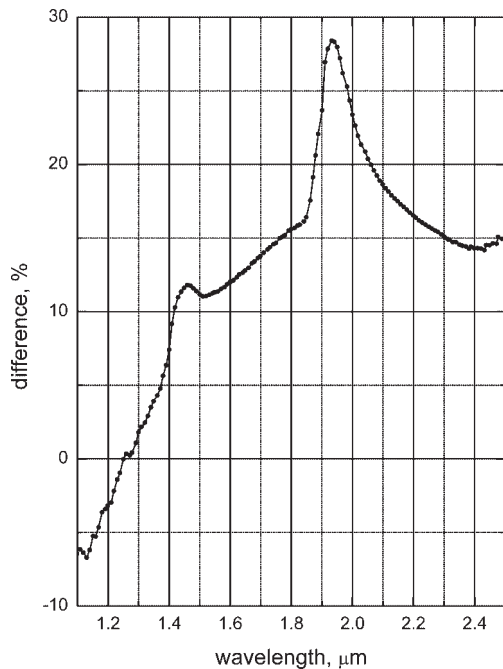


FIG. 7 The difference of spectra shown in Fig. 6 in percentages.

follows at $\lambda = 2 \mu\text{m}$, $a_{\text{ef}} = 4 \mu\text{m}$: $ka_{\text{ef}} = 4\pi \approx 12$ and $Y = 16\pi\chi$ or $Y \approx 0.06$, where we used $\chi \approx 0.0011$ at $\lambda = 2 \mu\text{m}$ (Ref. 32). The absolute values of Δ are smaller than 5% in the interval 1.18–1.28 μm .

CONCLUSIONS

A number of approximate formulae to calculate the reflective properties of semi-infinite turbid media were reviewed and compared with exact radiative transfer calculations. We find that the van de Hulst approximation gives the best results for the calculation of the spherical albedo r . It is interesting that the spherical albedo depends almost exclusively on the similarity parameter s . This means that light scattering media with different single scattering laws, but with the same values of s have almost the same spherical albedo (or the diffuse reflectance under diffuse illumination).

Simple relationships between the absorption spectra and correspondent spectra of reflected light are given for a specific case of bright turbid media. Results presented here can be used to improve modern color matching techniques.

ACKNOWLEDGMENTS

Authors are grateful to M. I. Mishchenko for providing the radiative transfer computer code used in this study.

1. Pierce PE, Marcus RT. Radiative transfer theory solid color-matching calculations. *Color Res Appl* 1997;22:72–87.
2. Kubelka P, Munk F. Ein Beitrag zur Optik der Farbanstriche. *Z Tech Phys* 1931;12:593–601.
3. Chandrasekhar S. *Radiative Transfer*. New York: Dover; 1960.

4. Philips-Invernizzi B, Dupont D, Caze C. Bibliographical review for reflectance of diffusing media. *Opt Eng* 2001;40:1082–1092.
5. Hapke B. *Theory of Reflectance and Emittance Spectroscopy*. Cambridge: Cambridge University Press; 1993.
6. Morel A, Gentili B. Diffuse reflectance of oceanic waters. III. Implication of bidirectionality for the remote-sensing problem. *Appl Opt* 1996;35:4850–4862.
7. Wozniak B. Mathematical spectral model of solar irradiance reflectance and transmittance by a wind-ruffled sea surface. Part 2: Modelling results and application. *Oceanologia* 1997;39:17–34
8. Mobley CD. Estimation of the remote-sensing reflectance from above-surface measurements. *Appl Opt* 1999;38:7442–7455.
9. Ambartsumian VA. On the scattering of light by a diffuse medium. *Dokl Akad Nauk SSSR* 1943;38:257–265. [*R Dokl Acad Sci USSR* 1943;38:229–232].
10. Sobolev VV. *Light Scattering in Planetary Atmospheres*. Oxford, England; Pergamon; 1975.
11. Kokhanovsky AA. *Light Scattering Media Optics*. Berlin: Springer-Praxis; 2004.
12. Mishchenko M, Dlugach J, Yanovitskij E, Zakharova N. Bidirectional reflectance of flat, optically thick particulate layers: An efficient radiative transfer solution and applications to snow and soil surfaces. *J Quant Spectrosc Radiat Transfer* 1999;63:409–430.
13. van de Hulst HC. The spherical albedo of a planet covered with a homogeneous cloud layer. *Astron Astrophys* 1974;35:209–214.
14. van de Hulst HC. *Multiple Light Scattering*, Vol. 2. London: Academic Press; 1980.
15. Dolin LS, Levin IM. *Handbook on the Theory of Underwater Vision*. Leningrad: Gidrometeoizdat; 1991.
16. Richards LW. The calculation of the optical performance of paint films. *J Paint Technol* 1970;42:276–286.
17. Mudgett PS, Richards LW. Multiple scattering calculations for technology. *Appl Opt* 1971;10:1485–1502.
18. Mie G. Beitrage zur Optik Truber Medien speziell kolloidaler Metallosungen. *Ann Phys* 1908;25:377–445.
19. Blewin WR, Brown WJ. Total reflectance of opaque diffusers. *J Opt Soc Am* 1962;52:1250–1255.
20. Bukata RP, Jerome JH, Kondratyev SA, Pozdnyakov DV. *Optical Properties and Remote Sensing of Inland and Coastal Waters*. New York: CRC Press; 1995.
21. Sokoletsky L. A comparative analysis of simple radiative transfer approaches for aquatic environments. In: *Proceedings of the 2004 ENVISAT Symposium*, Salzburg, Austria, September, 6–10, 2004.
22. Sokoletsky L. A comparative analysis of selected radiative transfer approaches for aquatic environments. *Appl Opt* 2005;44:136–148.
23. Bushmakova OV, Zege EP, Katsev IL. On asymptotic equations for brightness coefficients of optically thick light scattering layers. *Dokl Acad Sci BSSR* 1971;15:309–311.
24. Gordon HR. Simple calculation of the diffuse reflectance of the ocean. *Appl Opt* 1973;12:2803, 2804.
25. van de Hulst HC. *Light Scattering by Small Particles*. New York: Dover; 1981.
26. Debye P. Der Lichtdruck auf Kugeln von beliebigem Material. *Ann Phys* 1909;30:57–136.
27. Asano S, Yamamoto G. Light scattering by a spheroidal particle. *Appl Opt* 1975;14:29–49.
28. Mishchenko MI, Travis LD, Lacis AA. *Absorption, Scattering and Emission of Light by Small Particles*. New York: Cambridge University Press; 2002.
29. Kokhanovsky AA, Zege EP. Scattering optics of snow. *Appl Opt* 2004;43:1589–1602.
30. Allen E. Basic equations used in computer color matching. *J Opt Soc Am* 1966;56:1256–1259.
31. Allen E. Basic equations used in computer color matching. II. Tristimulus match, two-constant theory. *J Opt Soc Am* 1974;64:991–993.
32. Segelstein D. *The complex refractive index of water*. M.Sc. Thesis, University of Missouri, Kansas City, 1981.